Journal of
Materials Chemistry A

Materials for energy and sustainability

Accepted Manuscript

This article can be cited before page numbers have been issued, to do this please use: S. Zubkevich, G. R. Ragno, E. Tatsi, C. Botta, V. Berthé, L. Puchot, S. Turri, D. Schmidt, A. S. Shaplov and G. Griffini, *J. Mater. Chem. A*, 2026, DOI: 10.1039/D6TA01315E.

ROYAL SOCIETY OF CHEMISTRY

rsc.li/materials-a

View Article Online
DOI: 10.1039/D6TA01315E

ARTICLE

Covalent Functionalization of Polyhydroxyurethanes with Fluorescent Groups for Colorless Luminescent Solar Concentrators

Received 00th January 20xx,
Accepted 00th January 20xx

DOI: 10.1039/x0xx00000x

Sergei V. Zubkevich[†a], Gaia Roberta Ragno[†b], Elisavet Tatsi[†b], Chiara Botta[c], Vincent Berthé[a], Laura Puchot[a], Stefano Turri[b], Daniel F. Schmidt*[a], Alexander S. Shaplov*[a] and Gianmarco Griffini*[b]

Luminescent solar concentrators (LSCs) are attractive for building-integrated photovoltaics but require host matrices combining high transparency, stability, and sustainability. Here, half bio-based, isocyanate-free polyhydroxyurethanes (PHUs) are introduced as covalently functional host materials for transparent LSCs. Two aromatic fluorescent aldehydes based on fluorene and 8-hydroxycoumarin were synthesized and grafted onto a tailor-made PHU backbone via a facile post-synthetic modification strategy, yielding PHU_1-Flu and PHU_1-Coum with high degrees of functionalization (up to 80%). The resulting polymers were directly processed into thin-film LSCs by spin coating, acting simultaneously as host matrix and photoactive component. The devices exhibited excellent optical transparency and colour neutrality, with an average visible transmittance of ~90%, comparable to clear glass. Among the two systems, PHU_1-Flu showed superior performance, achieving external and internal photon efficiencies of 2.19% and 37.27%, respectively, a device efficiency of 0.34%, and a light utilization efficiency of 0.30%. By covalently immobilizing the luminophores, PHU-based LSCs inherently suppress dye migration and phase separation, addressing key stability limitations of conventional systems. These results demonstrate that bio-based PHUs represent not only sustainable but also functionally superior host matrices for durable and transparent LSCs.

Introduction

In the broad landscape of solar energy technologies, luminescent solar concentrators (LSCs) have emerged as a particularly attractive approach for integrating photovoltaics (PV) into the built environment. Their key advantages, such as tuneable optical properties (colour and transparency), lightweight design, and geometric flexibility, combined with their ability to efficiently harvest both direct and diffuse sunlight, render LSCs especially well-suited for such applications[1,2]. Together with device performance, another key factor in the design of LSC systems is their visual appearance, which is essential for the architectural and aesthetic integration of these technologies into buildings. Although power conversion efficiency remains vital for energy production, the aesthetic qualities of these systems are just as important for use in windows and facades, where high visible light transmittance may need to be prioritized over broad absorption (*viz.*, strong tinting) to ensure interior and external visual comfort[3]. The performance of LSCs is critically determined by the host matrix, which governs the photophysical behaviour of the embedded luminophores. Accordingly, the host material must satisfy several stringent requirements, including high optical transparency across the visible and near-infrared spectral ranges, an appropriate refractive index, and a homogeneous, defect-free surface to limit reflection and scattering losses[4,5].

Traditionally, polymethylmethacrylate (PMMA) and polycarbonate (PC) have been among the most widely used matrices for LSCs, largely due to their excellent optical transparency, well-matched refractive index, and commercial availability. PMMA, in particular, has become the benchmark material for LSC research, underpinning many of the most successful device demonstrations to date[2,6]. Nevertheless, despite methacrylates having long set the benchmark for LSC host matrices, increasing attention has been directed toward alternative polymer systems capable of extending device lifetimes, enabling novel fabrication strategies (e.g., coatings, flexible films), and better aligning with sustainability objectives. This shift has stimulated extensive exploration of bio-based and renewable materials for LSC applications[4,7]. Among biopolymers, poly-L-lactic acid (PLA)[8] has been investigated as a host matrix, demonstrating strong potential for optical applications and establishing itself as a viable alternative to PMMA. Similarly, silk fibroin (SF)[9] has emerged as a promising bio-based, water-processable, and environmentally benign material for LSCs. A recyclable and biocompatible alternative to conventional acrylic polymer emulsion-based matrices has been identified in lignocellulosic biomass, particularly cellulose nanocrystals (CNCs)[10]. Further bio-based host matrix candidates include two renewable polyesters[11] synthesized via a catalysed

[a] Luxembourg Institute of Science and Technology (LIST), Functional Polymeric and Particulate Materials Unit, 5 Avenue des Hauts-Fourneaux, L-4362 Esch-sur-Alzette, Luxembourg
[b] Department of Chemistry, Materials and Chemical Engineering "Giulio Natta", Politecnico di Milano, Piazza Leonardo da Vinci 32, Milano 20133, Italy
[c] Institute of Sciences and Chemical Technologies "Giulio Natta" (SCITEC) of CNR, Via A. Corti 12, 20133 Milano, Italy
* Corresponding authors: A.S.: alexander.shaplov@list.lu; D.S.: daniel.schmidt@list.lu; G.G.: gianmarco.griffini@polimi.it
† Equal contribution.

View Article Online
DOI: 10.1039/D6TA01715F

two-step melt polycondensation process: a homopolymer derived from diethyl 2,3:4,5-di-O-methylene galactarate (GxMe) and isosorbide, and a random copolymer of GxMe with 1,3-propanediol and dimethyl terephthalate. In addition, waterborne polymer dispersions[12] have been explored as sustainable host matrices, offering an organic solvent-free approach that mitigates environmental and health concerns associated with volatile and toxic organic compounds. Finally, proof-of-concept studies have demonstrated the feasibility of fabricating safe and sustainable LSCs using common food-grade materials such as isomalt as host matrices, combined with natural luminophores, including curcumin and riboflavin[13].

In this context, polyurethanes (PUs) represent a particularly versatile materials platforms[12,14–16], for the development of LSC, owing to their chemical tunability, optical transparency and ease of processing. Their structural flexibility enables the incorporation of a wide range of luminophores and photophysical design strategies. In this context, PU matrices have been combined with various fluorophore systems, including donor-acceptor architectures enabling efficient Förster resonance energy transfer (FRET)[15], intrinsically fluorescent backbones, and coumarin-based units acting both as emissive species and crosslinking agents[16]. In a recent example, carbon dots were incorporated into a PU hydrogel matrix as emissive centres for LSCs, demonstrating the ability of PU platforms to host nanostructured luminophores while maintaining optical transparency and processability[17]. Furthermore, the development of waterborne PU dispersions extends this versatility while offering a more sustainable, solvent-free approach that reduces the environmental and health concerns associated with volatile organic compounds[12]. Building on these efforts toward greener PU-based systems, their isocyanate-free analogues, polyhydroxyurethanes (PHUs)[18–20], provide an additional and highly attractive advantage by enabling greener synthetic routes that eliminate the use of toxic and hazardous isocyanates[21]. Importantly, PHUs can be synthesized from bio-based feedstocks and carbon dioxide, further strengthening their sustainability credentials[22,23]. Among the alternative synthetic strategies, the step-growth polyaddition of cyclic bis-carbonates (CBCs) with amines, leading to PHU formation, has emerged as one of the most extensively investigated and promising approaches[23]. A defining structural feature of PHUs obtained via this route is the presence of pendant hydroxyl groups along the polymer backbone. These hydroxyl functionalities offer unique opportunities for post-polymerization modification, allowing the deliberate incorporation of functional moieties and fine-tuning of the polymer's physical, chemical, and optical properties for targeted applications. Thus, beyond their sustainability advantages, PHUs can also potentially introduce a critical conceptual distinction compared with previously reported host matrices for LSCs. Unlike PMMA, polycarbonates, and other bio-based polymers discussed above, PHUs enable the covalent attachment of selected luminophores directly to the polymer backbone. This chemical bonding strategy fundamentally overcomes common challenges associated with physically blended luminophores, including limited compatibility with the host matrix, phase separation, dye aggregation, and long-term leaching.

Recently, we introduced a simple and scalable approach for the post-polymerization modification of tailor-made PHUs[24,25]. In this work, we demonstrated that rationally designed PHUs containing proximal hydroxyl groups along their backbone can be efficiently functionalized via a straightforward reaction with aldehydes, achieving modification efficiencies of up to 84%[24,25]. This facile strategy markedly increases the hydrophobicity of the resulting materials and effectively mitigates the impact of ambient humidity on their mechanical performance. Moreover, owing to the broad availability and structural diversity of functional aldehydes, this modification route provides a highly versatile platform for the introduction of application-specific functionalities into PHUs, thereby substantially expanding their scope for advanced and multifunctional material applications.

Building on these considerations, in the present work we synthesized two aromatic fluorescent aldehydes incorporating fluorene (**A_1**) and 8-hydroxycoumarin (**A_2**) moieties and employed them for the post-polymerization modification of a polyhydroxyurethane **PHU_1**, yielding two novel fluorescent polymers, **PHU_1-Flu** and **PHU_1-Coum** (Scheme 1). Both **PHU_1-Flu** and **PHU_1-Coum** were subsequently processed into thin-film luminescent solar concentrators (LSCs), in which they simultaneously function as the host matrix and the photoactive component. Finally, their photophysical characteristics, together with their photonic and photovoltaic (PV) responses, were systematically investigated in the context of highly transparent and colourless LSC devices.

View Article Online
DOI: 10.1039/D6TA01315E

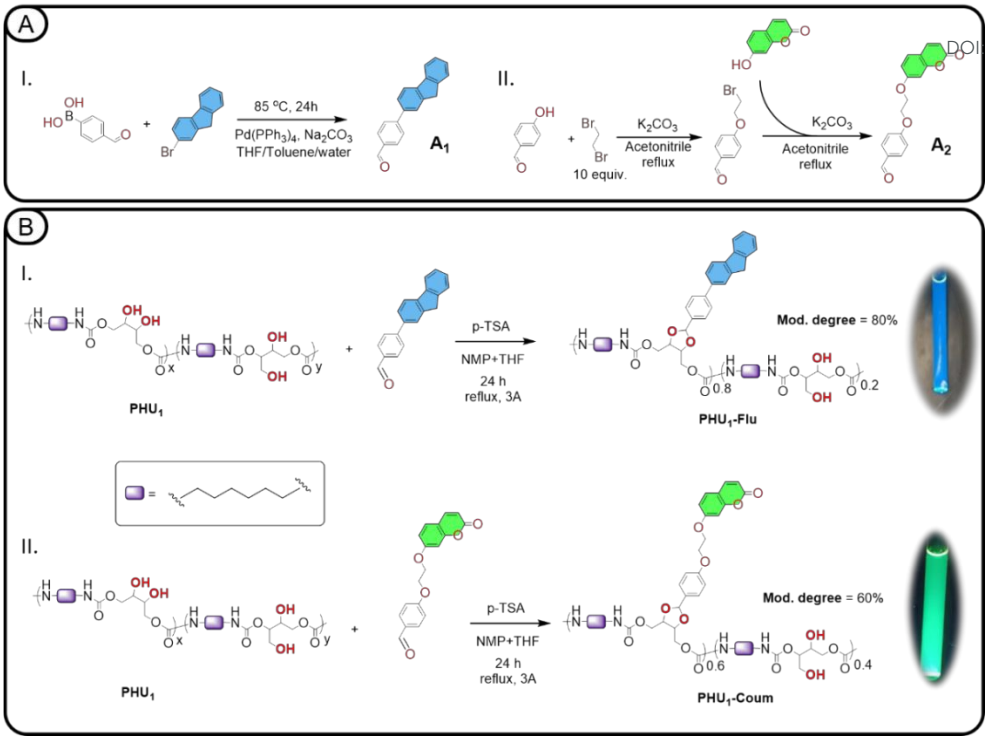

Scheme 1. (**A**) Synthetic routes for the preparation of fluorescent aldehydes $\mathbf{A_1}$ and $\mathbf{A_2}$; (**B**) Simplified scheme of **PHU$_1$-Flu** and **PHU$_1$-Coum** synthesis.

Results and discussion

Design and synthesis of fluorescent aldehydes

The work commenced with the rational design and synthesis of aldehydes $\mathbf{A_1}$ and $\mathbf{A_2}$ incorporating fluorescent moieties (Scheme 1). Among established luminophores, fluorene and 8-hydroxycoumarin[26] were selected owing to their molecular electronic structures, which efficiently fulfil the key photophysical requirements for strong and stable fluorescence. These include extended π-conjugation with intense π–π* transitions, rigid and largely planar frameworks that suppress non-radiative decay, high photostability, and favourable excited-state relaxation pathways.

In a subsequent step, the nature of the aldehyde functionality in $\mathbf{A_1}$ and $\mathbf{A_2}$ was carefully considered. Previous studies have demonstrated that maintaining a high glass-transition temperature (T_g) of the parent PHU after post-polymerization modification is more effectively achieved using aromatic aldehydes rather than their aliphatic counterparts[24,25]. Accordingly, aromatic aldehyde motifs were deliberately incorporated into the structures of $\mathbf{A_1}$ and $\mathbf{A_2}$.

Aldehyde $\mathbf{A_1}$ was synthesized in a single step from (4-formylphenyl)boronic acid and 2-bromo-9H-fluorene via a palladium-catalysed cross-coupling reaction, combining previously reported procedures for similar compounds[27–29] (Scheme 1A). In contrast, aldehyde $\mathbf{A_2}$ was prepared using a two-step protocol adapted from the literature[30,31]. The first step involved a Williamson etherification of the phenolic OH group with an α,ω-dibromoalkane to afford a mono-alkylated, bromo-terminated ether. In the second step, a subsequent Williamson O-alkylation with 7-hydroxy-2H-chromen-2-one yielded the bis-aryl ether $\mathbf{A_2}$. Compound $\mathbf{A_1}$ was initially recrystallized from hexane and subsequently from acetone, affording yellow crystals after drying. In contrast, $\mathbf{A_2}$ was recrystallized from an acetone/diethyl ether mixture, yielding a dark orange solid. The structure and purity of both aldehydes were confirmed by NMR spectroscopy (Fig. S1 and S4) and elemental analysis.

Differential scanning calorimetry (DSC) revealed that both $\mathbf{A_1}$ and $\mathbf{A_2}$ exhibited only melting transitions during the first heating cycle, with melting temperatures (T_m) of 194.6 and 160.1 °C, respectively (Fig. S2 and S5). Upon cooling, $\mathbf{A_1}$ readily recrystallized, showing a crystallization temperature (T_{cr}) of 174.8 °C. In contrast, $\mathbf{A_2}$, most likely due to the presence of a flexible spacer between the aromatic moieties, predominantly vitrified upon cooling and displayed crystallization only during the second heating cycle (Fig. S5).

Synthesis of PHU

In the PHU modification strategy previously developed by our group[25], the sole structural prerequisite for post-polymer modification is the presence and accessibility of two adjacent hydroxyl groups along the PHU backbone. This requirement can be fulfilled through the use of tailored bis(carbonate) monomers, such as bio-based erythritol dicarbonate. Accordingly, the parent polyhydroxyurethane (**PHU$_1$**) was synthesized via reactive extrusion by polyaddition of erythritol dicarbonate with hexamethylenediamine (Scheme 1B). The polymerization was conducted under optimized conditions (100

View Article Online
DOI: 10.1039/D5TA01315F

°C, 2.5 h) in the presence of 30 wt% N-methyl-2-pyrrolidone (NMP), which acts as a solubilizing medium and hydrogen-bond-disrupting agent, following our previously reported protocol[25]. The resulting PHU exhibited a number-average molecular weight of M_n = 12 500 g mol^{-1} with a broad molecular weight distribution, in good agreement with earlier reports[25,32]. ^{1}H NMR analysis of the **PHU$_1$** microstructure revealed a primary-to-secondary hydroxyl group ratio, OH(I):OH(II), of 25:75, as well as the presence of approximately 1.7 mol% urea linkages arising from side reactions during polyaddition[33,34].

Modification of PHUs

The next stage of this work focused on the modification of **PHU$_1$** with aldehydes **A$_1$** and **A$_2$** (Scheme 1B). While the aromatic character of **A$_1$** and **A$_2$** was intentionally selected to impart sufficiently high glass-transition temperatures (T_g) to the resulting modified polymers, **PHU$_1$-Flu** and **PHU$_1$-Coum**, thereby enabling the formation of mechanically stable polymer films, the same aromatic nature was anticipated to introduce additional challenges during the modification reaction. Indeed, the intrinsically lower reactivity of aromatic aldehydes has previously been shown to result in substantially reduced degrees of PHU functionalization compared to aliphatic analogues (43–61% versus 80–84%)[24,25]. This inherent limitation highlighted the need to further optimize the previously developed modification protocol in order to increase the achievable degree of functionalization when employing the aromatic aldehydes **A$_1$** and **A$_2$**.

Benzaldehyde was subsequently selected as a model aromatic substrate for systematic optimization studies (Fig. 1A; Supporting Information (SI), Section IV.2). When the original modification protocol was applied to **PHU$_1$** (Fig. 1B), a conversion of only 43% was achieved. To drive the equilibrium toward higher conversion, continuous removal of the reaction by-product (water) was required. Accordingly, the reaction setup was redesigned to include a Soxhlet extractor charged with 4 Å molecular sieves, and the solvent was changed from *N*-methyl-2-pyrrolidone (NMP) to tetrahydrofuran (THF). THF forms an azeotrope with water (boiling point 64 °C; 6.7% of water by weight[35]), thereby enabling efficient water removal under reflux conditions. Although the unmodified **PHU$_1$** polymer was insoluble in THF, the partially modified product (**PHU$_1$-Ph**) becomes soluble, as previously reported[25]. This solubility change facilitated reaction completion within 24 h, representing a substantial acceleration compared to the 72 h required under the original conditions. However, partial cross-linking of the resulting polymer was observed, likely due to the heterogeneous nature of the early-stage acetalization process. Despite the relatively low isolated yield (29%), the modification degree reached an unprecedented 93% (Fig. S6). To further refine the process, THF was replaced with acetonitrile, a solvent also capable of azeotrope formation with water (boiling point: 76.5 °C; 17.8% of water by weight[36]). This substitution afforded nearly identical outcomes, yielding 33% of the modified **PHU$_1$-Ph** with a 91% degree of modification (SI, Fig. S7). To suppress cross-linking, the modification process was rendered fully homogeneous by first dissolving **PHU$_1$** in NMP, followed by the gradual addition of THF (approximately 1:2 NMP:THF by volume) to avoid polymer precipitation. Under these optimized conditions, a high degree of modification of 91% was maintained (Fig. S8), while cross-linking was effectively suppressed, affording **PHU$_1$-Ph** in 93% yield as a fully soluble and well-defined polymer.

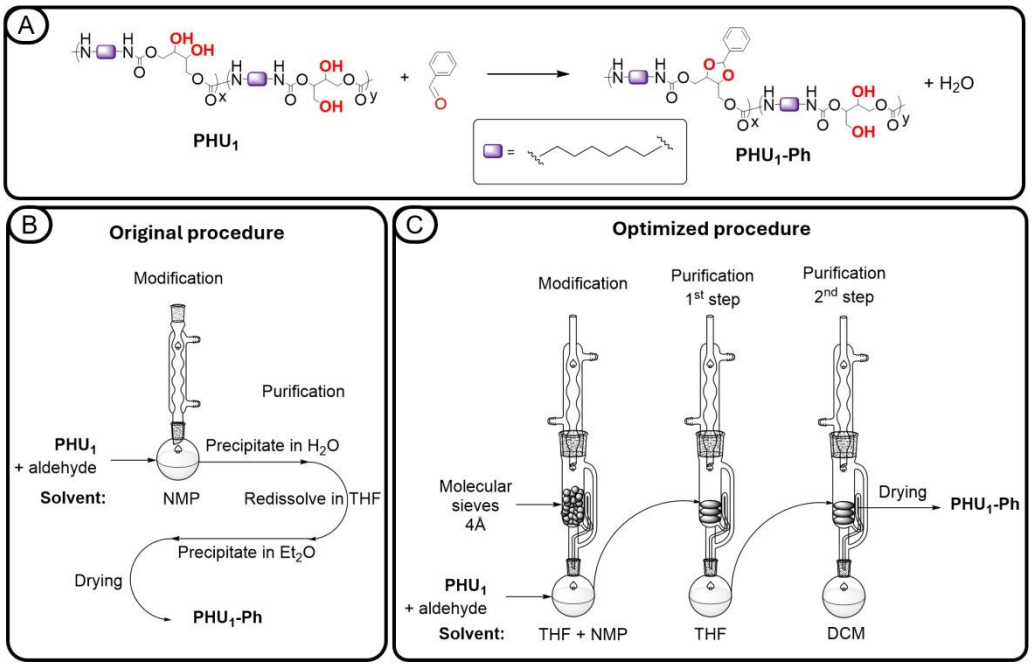

Figure 1. (**A**) Simplified scheme of **PHU$_1$** modification with benzaldehyde; (**B**) Original modification protocol reported in ref.[25]; (**C**) Optimized modification procedure developed in this work.

View Article Online
DOI: 10.1039/D5TA01745F

After optimization of the modification conditions using benzaldehyde, aldehydes **A_1** and **A_2** were subsequently employed for the modification of **PHU_1** (Fig. 1B). Upon completion of the reaction in the NMP/THF solvent mixture, the crude **PHU_1-Flu** and **PHU_1-Coum** polymers were initially precipitated in water following the standard protocol. However, owing to the markedly different solubility of **A_1** and **A_2** compared to benzaldehyde, ^{1}H NMR analysis of the crude **PHU_1-Flu** and **PHU_1-Coum** products revealed residual traces of **A_1** and **A_2**, respectively. In addition, the presence of an insoluble fraction was observed in the modified polymers, indicating partial cross-linking or incomplete modification. To ensure efficient isolation of well-defined products, a two-step purification procedure was further developed (Fig. 1C). In the first step, the modified polymers were subjected to Soxhlet extraction with boiling THF for 12 h. This treatment enabled the recovery of soluble, well-modified **PHU_1-Flu** and **PHU_1-Coum** together with any unreacted aldehyde, while poorly modified or cross-linked material remained in the Soxhlet thimble. In the second step, residual aldehyde was removed by subsequent Soxhlet extraction with dichloromethane (DCM) for 12 h. The purified **PHU_1-Flu** and **PHU_1-Coum** polymers were then dried under vacuum and further characterized. The structure and purity of **PHU_1-Flu** and **PHU_1-Coum** were confirmed by ^{1}H (SI, Figs. S9 and S13) and ^{13}C NMR spectroscopy (SI, Figs. S10 and S14). The degrees of modification, determined from ^{1}H NMR spectra, were found to be 80% for **PHU_1-Flu** and 60% for **PHU_1-Coum** (Table 1). Gel permeation chromatography (GPC) analysis of the modified polymers revealed number-average molecular weights (M_n) in the range of 17–22 kDa, with GPC traces exhibiting a shoulder in the high-molar-mass region (Fig. S17). However, these values and the apparent increase in molecular weight should be interpreted with caution. First, GPC calibration was performed using PMMA standards, which differ significantly in chemical structure from PHU. Second, the introduction of bulky side groups via covalent bonding substantially alters the polymer chain conformation and hydrodynamic volume.

The synthesized PHUs exhibit relatively broad molar mass distributions (Đ = 6.4–12.9, Table 1, Fig. S17), exceeding the ideal value of 2 predicted by Flory's theory for step-growth polymerization. However, this prediction assumes equal functional group reactivity and homogeneous reaction conditions, which are not fully met in the present system. The polymerization is carried out under reactive extrusion conditions starting from partially heterogeneous solid precursors (EDC and HMDA), and the progressive formation of hydroxyl-rich PHU chains alters the local environment, including hydrogen bonding and solvation effects, thus affecting reactivity during the course of the reaction. Such deviations from ideal behaviour are commonly reported for PHU systems[37,38]. In addition, post-functionalization with fluorescent aldehydes (60–80% modification degree) further alters polymer polarity and interactions, which can influence the apparent dispersity measured by GPC. Finally, partial removal of low-molar-mass oligomers during purification, particularly in the case of PHU1-Coum (lower yield), may also contribute to the observed differences in dispersity.

Table 1. Properties of PHU polymers modified with fluorescent aldehydes.

Sample	Modification degree, %[a]	M_n, g mol^{-1}[b]	$Đ = M_w/M_n$[b]	T_{onset}, °C[c]	T_g, °C[d]	T_m, °C[d]
PHU_1-Flu	80	17000	12.9	235	97	153
PHU_1-Coum	60	22400	6.4	220	65	147

[a] Calculated from ^{1}H NMR; [b] Determined by GPC in 0.1M $Li(CF_3SO_2)_2N$ solution in DMF at 50 ˚C with PMMA standards; [c] Determined by TGA in air at a heating rate of 5 ˚C min^{-1}; [d] Determined by DSC at a heating rate of 5 ˚C min^{-1}.

Thermal properties of modified PHUs

The thermal stability of the modified PHUs was evaluated using thermogravimetric analysis (TGA) (Table 1, SI, Fig. S12 and S16). Both **PHU_1-Flu** and **PHU_1-Coum** exhibited onset decomposition temperatures above 220 °C in air, indicating sufficient thermal stability for applications at elevated temperatures. Differential scanning calorimetry (DSC) was then employed to examine their thermal transitions (SI, Fig. S11 and S15). Both **PHU_1-Flu** and **PHU_1-Coum** showed two distinct thermal transitions, which were assigned to the glass transition temperature (T_g) and the melting transition (T_m), occurring at approximately 65–97 °C and ~150 °C, respectively (Table 1). The presence of well-defined and reproducible melting and crystallization transitions is indicative of semicrystalline behaviour, in agreement with previous observations reported for PHUs modified with aromatic aldehydes [24,25].

Photophysical properties of modified fluorescent PHUs

The photophysical properties of the modified PHU polymers were first investigated by UV-vis absorption and fluorescence spectroscopy, both in solution and in the solid state (as a thin film). Solution measurements were performed on dilute polymer solutions in DMF (≈10^{-7} M), while thin films were prepared by spin-coating 10 wt% PHU solutions in DMF onto glass substrates at 900 rpm for 60 s, yielding film thicknesses of approximately 0.7 µm for **PHU_1-Flu** and 0.5 µm for **PHU_1-Coum**. In solution (Fig. 2A), **PHU_1-Flu** exhibited two absorption maxima at 297 and 310 nm and an emission maximum centred at 351 nm. In contrast, **PHU_1-Coum** showed absorption and emission maxima at 320 and 394 nm, respectively. Upon transitioning from solution to thin films, a slight red shift of the emission maxima was observed for both polymers (Fig. 2B), which can be attributed to enhanced intermolecular interactions in the solid state, the possible formation of aggregated species, and reabsorption processes[39,40]. As shown in Fig. 2B, the emission maxima of **PHU_1-Flu** and **PHU_1-Coum** were shifted to 368 and 410 nm, respectively, corresponding to red shifts of 17 nm (0.16 eV) and 16 nm (0.12 eV). In addition, the emission bands in the

View Article Online
DOI: 10.1039/D5TA01515E

solid state were noticeably broader than those observed in solution, particularly for **PHU$_1$-Flu** (Fig. 2B, dashed blue line). This broadening is likely related to the relatively high dispersity of the PHUs, as increased *Đ* can introduce additional energetic disorder, leading to a wider distribution of emissive states[41,42]. Consequently, this energetic heterogeneity manifests itself as an increased emission bandwidth. Furthermore, higher apparent Stokes shifts (≈80 nm) were observed in the thin films compared to solution. This effect can be attributed not only to changes in the local environment and solid-state interactions, but also to self-absorption processes, which may contribute to the red-shift and broadening of the emission. While such effects can enhance reabsorption processes, the measured radiative overlap values remain moderate (Table S2), indicating that reabsorption losses remain limited.[43,44]

To assess the effect of covalent incorporation, the corresponding fluorophores (A_1 and A_2) were also physically dispersed in a host-guest fashion in a conventional PMMA matrix, widely used in LSC fabrication, at concentrations matching those of the PHU-based systems. Under comparable preparation conditions, the covalently functionalized PHU systems exhibited improved solid-state emission properties relative to the corresponding PMMA-based films, as confirmed by photoluminescence quantum yield, fluorescence lifetime, and LSC efficiency measurements (see Supporting Information, Table S1 and Fig. S19–S20). These results suggest that the covalent attachment of the fluorophores to the PHU backbone provides a more favourable and restricted local environment for emission compared to simple physical dispersion in the polymer matrix.

Additional photostability measurements were also performed on both PHU-based and host-guest PMMA-based systems under prolonged AM 1.5G irradiation. The covalently functionalized PHU films retained more stable optical properties over time, whereas the corresponding PMMA-based systems exhibited a more pronounced, continuous decrease in photoluminescence intensity under identical irradiation conditions (see Supporting Information, Section V.2)

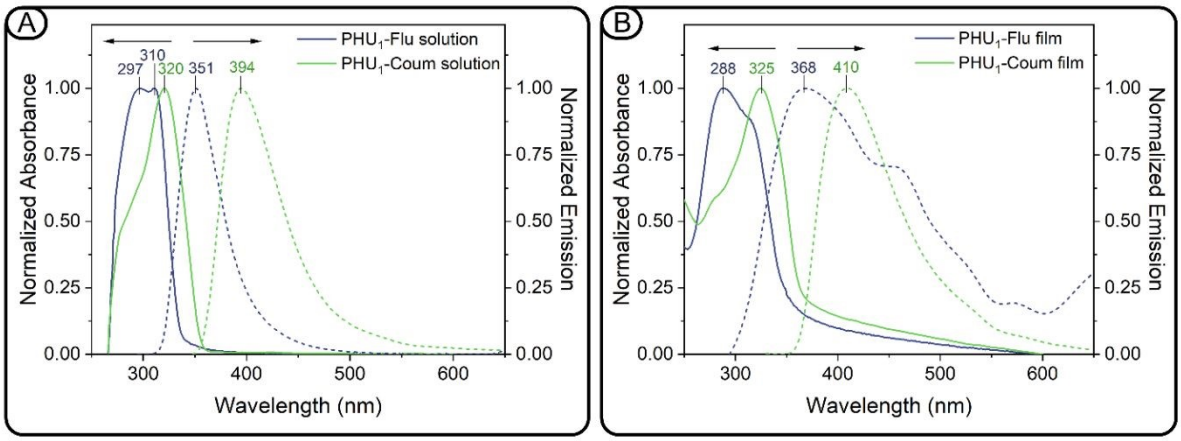

Figure 2. UV-vis absorption and fluorescence emission spectra of **PHU$_1$-Flu** and **PHU$_1$-Coum** polymers measured in (**A**) solution (10^{-7} M in DMF) and (**B**) thin films. Emission spectra were recorded using excitation wavelengths of 290 and 325 nm for **PHU$_1$-Flu** and **PHU$_1$-Coum** in solution, and 300 and 320 nm, respectively, in the solid state.

Characterization of modified PHU-based luminescent solar concentrators (LSCs)

Based on the results discussed above, LSC devices were fabricated by preparing 10 wt% solutions of **PHU$_1$-Flu** and **PHU$_1$-Coum** in DMF and depositing them onto N-BK7 high-optical-quality glass substrates (5.0 × 5.0 × 0.6 cm³) by spin coating (900 rpm, 60 s). The visual appearance of LSCs is a key factor for their successful integration into architectural environments. Accordingly, the aesthetic quality of the devices was quantitatively assessed using two complementary optical metrics: the average visible transmittance (AVT), which evaluates device transparency as perceived by the human eye under photopic conditions, and the CIELAB chromaticity coordinates (a*, b*), which quantify colour neutrality relative to natural daylight. As shown in the inset of Fig. 3A, the fabricated LSCs exhibited a highly transparent and visually colourless appearance. This observation was corroborated by optical transmittance measurements (Fig. 3A), which revealed AVT values of approximately 90%, comparable to those of conventional residential clear windows[45,46]. Details of the AVT calculation are provided in the Supporting Information (Section VI.4, Equation S10). Furthermore, the chromaticity coordinates of both PHU-based LSCs overlapped with the central neutral region of the CIE 1931 chromaticity diagram (x = 0.35, y = 0.36; Fig. 3B), thereby confirming the essentially colourless nature of the devices.

View Article Online
DOI: 10.1039/D6TA01315E

ARTICLE

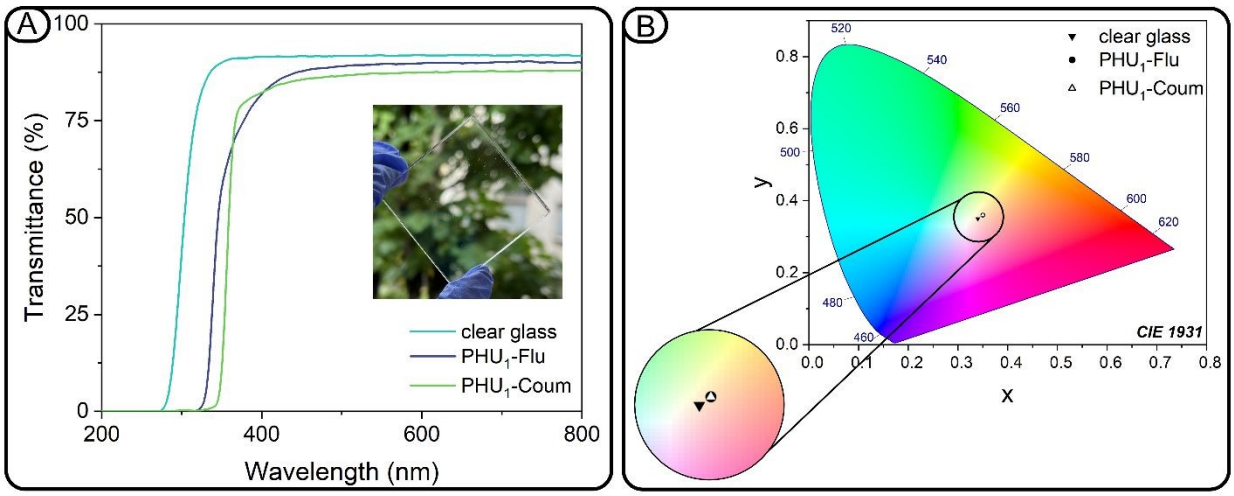

Figure 3. (**A**) Optical transmittance spectra of **PHU$_1$-Flu** and **PHU$_1$-Coum** compared with clear glass; inset: photograph of a representative LSC demonstrating high optical transparency. (**B**) CIE 1931 chromaticity diagram of **PHU$_1$-Flu** and **PHU$_1$-Coum** compared with clear glass.

To evaluate the photonic response of the modified PHU-based LSCs, the devices were characterized in the 300-750 nm wavelength range under standard solar illumination (AM 1.5G). Among the investigated systems, **PHU$_1$-Flu** exhibited superior performance in terms of both external photon efficiency (η_{ext}) and internal photon efficiency (η_{int})[47], yielding values of 2.19% and 37.27%, respectively. These values were notably higher than those obtained for **PHU$_1$-Coum**, which reached η_{ext} and η_{int} values of 1.67% and 28.37%, respectively. By contrast, the absorption efficiency (η_{abs}) was comparable for both polymers, with values of approximately 8%. The observed differences in device performance can be primarily attributed to the higher photoluminescence quantum yield (PLQY) of **PHU$_1$-Flu** relative to **PHU$_1$-Coum** (see SI, Section V), which directly impacts photon conversion and emission efficiency. To further assess the practical photovoltaic (PV) output, the LSCs were coupled to monocrystalline silicon PV cells connected in series (experimental details in SI, Section VI.3, a representative photograph and a scheme of the LSC-PV assembly is provided in SI, Fig. S24). Consistent with the photonic efficiency results, the **PHU$_1$-Flu** -based device delivered the highest PV response, achieving a short-circuit current (I_{sc}) of 5.63 mA and an overall device power conversion efficiency (η_{dev}) of 0.34%. In comparison, the **PHU$_1$-Coum** device exhibited slightly lower values (I_{sc} =5.10 mA and η_{dev}=0.30%).

Finally, the light utilization efficiency (LUE) was introduced as a comprehensive figure of merit that captures the trade-off between the aesthetic quality of the LSCs, quantified by the AVT, and their functional PV performance, quantified by η_{dev}. In line with the above results, **PHU$_1$-Flu** exhibited a marginally higher LUE (0.30%) than **PHU$_1$-Coum** (0.26%). When benchmarked against previously reported colourless or semi-transparent LSCs based on a variety of polymer matrices, the η_{dev} and LUE values achieved in this work are fully competitive with the current state of the art. Notably, the performance of the present PHU-based LSCs compares favourably with that of transparent polymer-based devices employing UV- or NIR-absorbing luminophores, as summarized in Table S6. Additional details on the calculation procedures and experimental methodologies employed for LSC device characterization are provided in the Supporting Information (Section VI).

Conclusions

Overall, the simple and scalable post-polymerization modification strategy for tailor-made PHUs previously introduced by our group was successfully extended to the incorporation of fluorescent aldehydes, thereby highlighting the potential of bio-based, isocyanate-free polyhydroxyurethanes as sustainable and versatile materials for luminescent solar concentrators (LSCs).

In particular, a tailor-made polyhydroxyurethane was successfully modified through the covalent incorporation of fluorescent aldehydes based on fluorene and 8-hydroxycoumarin, yielding two novel fluorescent polymers **PHU$_1$-Flu** and **PHU$_1$-Coum**. The resulting materials were directly spin-coated onto high-optical-quality glass substrates, acting simultaneously as both the host matrix and the active

luminescent component in LSC devices. The fabricated LSCs exhibited excellent optical transparency and colour neutrality, with average visible transmittance values of approximately 90% and chromaticity coordinates located in the neutral region, rendering them well-suited for architectural integration. Among the investigated systems, **PHU_1-Flu** demonstrated superior photonic and photovoltaic performance, achieving higher external and internal photon efficiencies (2.19% and 37.27%, respectively) compared to **PHU_1-Coum**, as well as an enhanced device efficiency (η_{dev} = 0.34%). Consistently, **PHU_1-Flu** also displayed a slightly higher light utilization efficiency (0.30%), reflecting a favourable balance between optical transparency and energy conversion efficiency. Importantly, the PHU-based LSCs introduced in this study inherently suppress luminophore migration and phase stratification within the polymer matrix as a consequence of chromophore covalent bonding, thereby enhancing optical stability, device durability, and expected operational lifetime. Consequently, bio-based, isocyanate-free PHUs should be regarded not merely as sustainable alternatives to conventional acrylic or carbonate matrices, but as functionally superior host materials that offer a robust solution to key stability challenges in LSC devices.

Author contributions

Sergei V. Zubkevich – Investigation, Visualization, Data curation, Formal Analysis, Writing – original draft; Gaia Roberta Ragno – Investigation, Data curation, Formal Analysis,; Elisavet Tatsi – Methodology, Data curation, Formal Analysis, Writing – original draft ; Chiara Botta – Investigation, Formal analysis, Data curation; Vincent Berthé – Resources, Funding Acquisition and Project administration; Laura Puchot – Formal Analysis, Validation; Stefano Turri – Methodology, Formal analysis; Writing – review & editing; Daniel F. Schmidt – Writing – review & editing, Supervision; Alexander S. Shaplov – Project administration, Supervision, Writing – review & editing; Gianmarco Griffini – Conceptualization, Methodology, Supervision, Funding acquisition, Writing – review & editing.

Conflicts of interest

There are no conflicts to declare.

Data availability

The data supporting this article have been included as part of the Supplementary Information.

Supplementary Information contains a description of materials and methods, synthesis and characterization of aldehydes **A_1** and **A_2**, synthesis and characterization of PHU polymers, photophysical properties of modified PHU polymers, and optical and Photovoltaic Characterization of thin-film modified PHU-based devices. Additional references have been cited in SI.

Acknowledgements

This work was supported by the European Commission through the Marie Skłodowska-Curie Individual Fellowship (MSCA-PF-EF) project "SPRUT" (Grant No. 101066839) under the HORIZON-TMA-MSCA-PF-EF programme. Additional funding was provided by the Luxembourg National Research Fund (FNR) within the project SAFFIA (Agreement No. INTER/MERA20/15020254), Italian Ministry of University and Research (MUR) through the PRIN 2022 programme (Grant No. 2022BREBFN, project NIR+) and by the Cariplo Foundation (Ref. No. 2023-1656, project PHASMA).

References

1 B. S. Richards and I. A. Howard, *Energy Environ. Sci.*, 2023, **16**, 3214–3239.

2 S. Castelletto and A. Boretti, *Nano Energy*, 2023, **109**, 108269.

3 P. Moraitis, G. van Leeuwen and W. van Sark, *Materials*, 2019, **12**, 885.

4 G. Griffini, *Front. Mater.*, 2019, **6**,3214-3239.

5 M. Zettl, O. Mayer, E. Klampaftis and B. S. Richards, *Energy Technology*, 2017, **5**, 1037–1044.

6 Y. Li, X. Zhang, Y. Zhang, R. Dong and C. K. Luscombe, *J. Polym. Sci. A Polym. Chem.*, 2019, **57**, 201–215.

7 M. A. Hernández-Rodríguez, S. F. H. Correia, R. A. S. Ferreira and L. D. Carlos, *J. Appl. Phys.*, 2022, **131**, 140901.

8 V. Fattori, M. Melucci, L. Ferrante, M. Zambianchi, I. Manet, W. Oberhauser, G. Giambastiani, M. Frediani, G. Giachi and N. Camaioni, *Energy Environ. Sci.*, 2011, **4**, 2849.

9 M. Melucci, M. Durso, L. Favaretto, M. L. Capobianco, V. Benfenati, A. Sagnella, G. Ruani, M. Muccini, R. Zamboni, V. Fattori and N. Camaioni, *RSC Adv.*, 2012, **2**, 8610.

10 F. I. Chowdhury, C. Dick, L. Meng, S. M. Mahpeykar, B. Ahvazi and X. Wang, *RSC Adv.*, 2017, **7**, 32436–32441.

11 T. A. Geervliet, I. Gavrila, G. Iasilli, F. Picchioni and A. Pucci, *Chem. Asian J.*, 2019, **14**, 877–883.

12 P. Minei, G. Iasilli, G. Ruggeri and A. Pucci, *Coatings*, 2020, **10**, 655.

13 A. Picchi, A. Pucci and M. Carlotti, *J. Chem. Educ.*, 2023, **100**, 4559–4566.

14 J. Bai, Y. Zhai, X. Li, M. Hao, W. Ren, M. He and Z. Li, *Opt. Mater. (Amst).*, 2025, **167**, 117301.

15 E. Tatsi, M. De Marzi, L. Mauri, A. Colombo, C. Botta, S. Turri, C. Dragonetti and G. Griffini, *Macromol. Rapid Commun.*, 2024, **45**, 1–12.

16 G. Fortunato, E. Tatsi, F. Corsini, S. Turri and G. Griffini, *ACS Appl. Polym. Mater.*, 2020, **2**, 3828–3839.

17 W. Li, J. Lin, J. Li, Q. Jing, N. Ren, J. Xiao, H. Zhao, Y. Song and A. Vomiero, *Nano Energy*, 2026, **148**, 111674.

18 L. Maisonneuve, O. Lamarzelle, E. Rix, E. Grau and H. Cramail, *Chem. Rev.*, 2015, **115**, 12407–12439.

19 G. Rokicki, P. G. Parzuchowski and M. Mazurek, *Polym. Adv. Technol.*, 2015, **26**, 707–761.

20 A. Cornille, R. Auvergne, O. Figovsky, B. Boutevin and S. Caillol, *Eur. Polym. J.*, 2017, **87**, 535–552.

21 I. Kimber, R. J. Dearman and D. A. Basketter, *Journal of Applied Toxicology*, 2014, **34**, 1073–1077.

22 S. Schmidt, F. J. Gatti, M. Luitz, B. S. Ritter, B. Bruchmann and R. Mülhaupt, *Macromolecules*, 2017, **50**, 2296–2303.

23 M. Ghasemlou, F. Daver, E. P. Ivanova and B. Adhikari, *Eur. Polym. J.*, 2019, **118**, 668–684.

24 A. S. Shaplov, D. Schmidt and S. Zubkevich, LU503467B1, 2024.

25 S. V Zubkevich, M. Makarov, R. Dieden, L. Puchot, V. Berthé, S. Westermann, A. S. Shaplov and D. F. Schmidt, *Macromolecules*, 2024, **57**, 2385–2393.

26 A. P. de Silva, H. Q. N. Gunaratne, T. Gunnlaugsson, A. J. M. Huxley, C. P. McCoy, J. T. Rademacher and T. E. Rice, *Chem. Rev.*, 1997, **97**, 1515–1566.

27 L. Li, R. Matsuda, I. Tanaka, H. Sato, P. Kanoo, H. J. Jeon, M. L. Foo, A. Wakamiya, Y. Murata and S. Kitagawa, *J. Am. Chem. Soc.*, 2014, **136**, 7543–7546.

28 Q. Xie, J. Li, X. Wen, Y. Huang, Y. Hu, Q. Huang, G. Xu, Y. Xie and Z. Zhou, *Carbohydr. Res.*, 2022, **512**, 108516.

29 Z. Zhou, Y. Yuan, Y. Xie and M. Li, *Catal. Letters*, 2018, **148**, 2696–2702.

30 M. J. Brites, C. Santos, S. Nascimento, B. Gigante and M. N. Berberan-Santos, *Tetrahedron Lett.*, 2004, **45**, 6927–6930.

31 S. Cao, Y. Xia, J. Shao, B. Guo, Y. Dong, I. A. B. Pijpers, Z. Zhong, F. Meng, L. K. E. A. Abdelmohsen, D. S. Williams and J. C. M. van Hest, *Angew. Chem. Int. Ed.*, 2021, **60**, 17629–17637.

32 S. V Zubkevich, A. D. Sarma, O. N. Antzutkin, R. Dieden, V. Berthe, S. Westermann, A. S. Shaplov and D. F. Schmidt, *Chemistry of Materials*, 2025, **37**, 7049–7063.

33 F. Magliozzi, G. Chollet, E. Grau and H. Cramail, *ACS Sustain. Chem. Eng.*, 2019, **7**, 17282–17292.

34 A. Bossion, R. H. Aguirresarobe, L. Irusta, D. Taton, H. Cramail, E. Grau, D. Mecerreyes, C. Su, G. Liu, A. J. Müller and H. Sardon, *Macromolecules*, 2018, **51**, 5556–5566.

35 S. Xu and H. Wang, *Chemical Engineering Research and Design*, 2006, **84**, 478–482.

36 S. Chaudhari, Y. Kwon and M. Shon, *Bull. Korean Chem. Soc.*, 2019, **40**, 220–229.

37 F. Monie, T. Vidil, E. Grau, B. Grignard, C. Detrembleur and H. Cramail, *Macromolecules*, 2024, **57**, 8877−8888.

38 A. Datta Sarma, S. V. Zubkevich, F. Addiego, D. F. Schmidt, A. S. Shaplov and V. Berthé, *Macromolecules*, 2024, **57**, 3423–3437.

39 J. Donovalová, M. Cigáň, H. Stankovičová, J. Gašpar, M. Danko, A. Gáplovský and P. Hrdlovič, *Molecules*, 2012, **17**, 3259–3276.

40 H. Zhang, T. Li, T. Ma, B. Liu, J. Ren, J. Lin, M. Yu, L. Xie and D. Lu, *The Journal of Physical Chemistry C*, 2019, **123**, 27317–27326.

41 A. Menon, H. Dong, Z. I. Niazimbetova, L. J. Rothberg and M. E. Galvin, *Chemistry of Materials*, 2002, **14**, 3668–3675.

42 K. Schötz, F. Panzer, M. Sommer, H. Bässler and A. Köhler, *Mater. Horiz.*, 2023, **10**, 5538–5546.

43 L. R. Wilson, B. C. Rowan, N. Robertson, O. Moudam, A. C. Jones and B. S. Richards, *Appl. Opt.*, 2010, **49**, 1651.

44 M. G. Debije and P. P. C. Verbunt, *Adv. Energy Mater.*, 2012, **2**, 12–35.

45 C. J. Traverse, R. Pandey, M. C. Barr and R. R. Lunt, *Nat. Energy*, 2017, **2**, 849–860.

46 C. Yang, D. Liu, M. Bates, M. C. Barr and R. R. Lunt, *Joule*, 2019, **3**, 1803–1809.

47 M. G. Debije, R. C. Evans and G. Griffini, *Energy Environ. Sci.*, 2021, **14**, 293–301.

The data supporting this article have been included as part of the Supplementary Information.

View Article Online
DOI: 10.1039/D6TA01315E